ASEAN Engineering Journal

Full Paper

DESIGNING OF DYNAMIC SURFACE CONTROL BASED ON BACKSTEPPING TECHNIQUE FOR SERIES ELASTIC ACTUATOR ROBOT

Minh-Duc Duong*, Thanh-Tung Tran

School of Electrical & Electronic Engineering, Hanoi University of Science and Technology, Vietnam

Article history
Received
14 March 2023
Received in revised form
16 July 2023
Accepted
17 July 2023
Published online
29 February 2024

*Corresponding author
duc.duongminh@hust.edu.vn

Graphical abstract

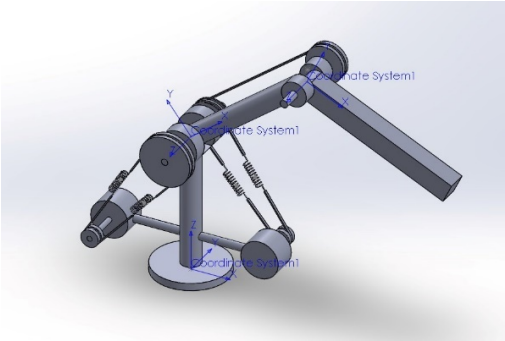

Abstract

Serial elastic actuators have gained significant attention in robotics research due to their ability to meet safety requirements in physical interactions between humans and robots. However, one problem of series elastic actuator is the oscillation of the robot due to the flexibility of the robotic joints leading to a decline in the accuracy of the robot's position control. In this paper, a dynamic surface control algorithm based on the backstepping technique for the position control of serial elastic actuator robot is proposed to overcome the oscillation problem. In addition, the proposed control algorithm has been proved to be stable and robust. The simulation results clearly demonstrate the effectiveness of the proposed method.

Keywords: Series elastic actuator, backstepping control, dynamic surface control, nonlinear system design.

1.0 INTRODUCTION

In recent years, motion control of elastic joint robot has attracted the attention of researchers. Series elasticity has been recognized as a crucial aspect for force control in robotics research [1]–[6], as well as for energy storage and release during activities such as running or hopping [7]–[9]. In this actuator, known as a Series Elastic Actuator (SEA) [10], there is an intentional spring in series with the transmission and the actuator output. While the spring somewhat reduces bandwidth, it can also help to reduce the output impedance of the actuator and act as a mechanical low-pass filter for shocks, particularly in force control applications.

The series elastic actuator are increasingly largely applied and popular in industrial activities and for many related applications related humans such as requiring high precision, reteration and also human activities that cannot be participated in. In industrial applications, SEAs offer several key benefits, including the reduction of reflected inertia, greater tolerance to impact loads, passive mechanical energy storage, low mechanical output impedance, and increased peak power output [11]. In addition, in human robot interaction, the SEA system is used a lot in rehabilitation robots. SEA helps compensate for the foce when interacting with humans and is safe to use [12].

Various control algorithms have been introduced to control series elastic actuator robotic systems and achieve certain efficiency [13], [14]. Control algorithms are divided into two groups of solutions: linear control and nonlinear control. Among them, nonlinear control methods are more widely used in robot control, such as sliding mode cotrol [15], [16], backstepping control [17] for position control, adaptive Li-Slotine based backstepping control [18]; and passivity control [19], [20], demultiplexing control [21] for force/impedance control. For position control, sliding mode control and backstepping control are an effective control techniques and widely applied to various system including SEA robot. However, the controller contains the derivative elements that causes the "explosion of terms" problem. To overcome this, in this paper, a dynamic surface controller (DSC) based on backstepping technique is proposed. The controller is proven to ensure the stability and robustness of the system. Not only that, the proposed conroller also deals

with limited disadvantages such as "explosion of terms" that causes a high control input when the derivative changes rapidly of the conventional backstepping method.

2.0 DYNAMICAL MODEL OF THE SEA

For simplicity, in this paper, we have used a two – link SEA robot model as in Figure 1. The robot's elastic mechanism is designed based on the elasticity of elastic tendons and springs, which is convenient for calculation and control. The results of the paper are fully extendable to N – joints robot.

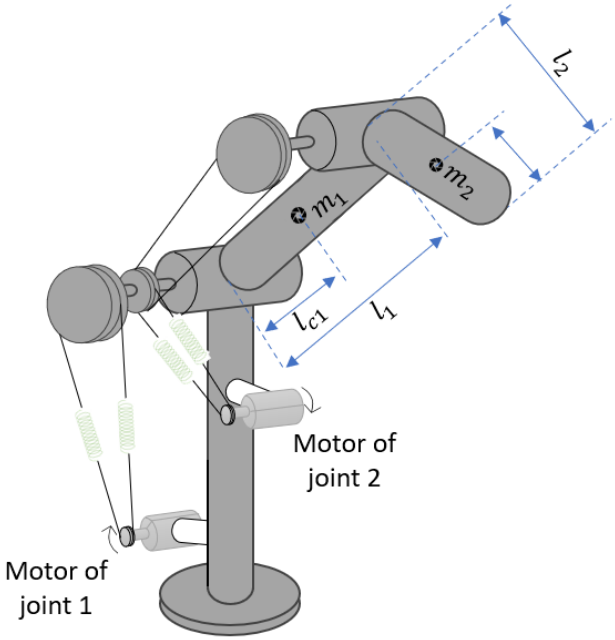

Figure 1. Robot system model of SEA

Define $\overline{\boldsymbol{q}} = \begin{bmatrix} q_1 \\ q_2 \end{bmatrix}$ is the joint angle vector of the robot arm, $\overline{\boldsymbol{\theta}} = \begin{bmatrix} \theta_1 \\ \theta_2 \end{bmatrix}$ represents the vector of motor angles, the kinetic energy of the system is given by:

$$K_E = \frac{1}{2}\dot{\overline{\boldsymbol{q}}}^T \boldsymbol{D}\dot{\overline{\boldsymbol{q}}} + \frac{1}{2}\dot{\overline{\boldsymbol{\theta}}}^T \boldsymbol{J}\dot{\overline{\boldsymbol{\theta}}} \tag{1}$$

where $\boldsymbol{D} = \boldsymbol{D}(\overline{\boldsymbol{q}}), \boldsymbol{J} = \begin{bmatrix} J_1 & 0 \\ 0 & J_2 \end{bmatrix}$ are the rotational inertias of the link and motor, respectively.

The potential energy is comprised of both the spring potential energy and the gravitational potential energy:

$$P_E = p(\overline{\boldsymbol{q}}) + \frac{1}{2}(\overline{\boldsymbol{q}} - \overline{\boldsymbol{\theta}})^T K(\overline{\boldsymbol{q}} - \overline{\boldsymbol{\theta}}) \tag{2}$$

where $\boldsymbol{K} = \begin{bmatrix} K_1 & 0 \\ 0 & K_2 \end{bmatrix}$ is the spring stiffness, and the potential energy is calculated as $p(\overline{\boldsymbol{q}}) = (m_1 l_{c1} + m_2 l_1) g sinq_1 + m_2 l_{c2} \sin(q_1 + q_2)$.

Forming the Lagrange function $L = K_E - P_E$, the equation of motion is found from the Euler – Lagrange equation as [22]:

$$\begin{aligned} \boldsymbol{D}\ddot{\overline{\boldsymbol{q}}} + \boldsymbol{C}\dot{\overline{\boldsymbol{q}}} + \boldsymbol{G} &= \boldsymbol{K}(\overline{\boldsymbol{\theta}} - \overline{\boldsymbol{q}}) \\ \boldsymbol{J}\ddot{\overline{\boldsymbol{\theta}}} + \boldsymbol{K}(\overline{\boldsymbol{\theta}} - \overline{\boldsymbol{q}}) &= \overline{\boldsymbol{u}} \end{aligned} \tag{3}$$

where $\boldsymbol{D} = \boldsymbol{D}(\overline{\boldsymbol{q}})$ is the link inertia matrix, $\boldsymbol{C} = \boldsymbol{C}(\overline{\boldsymbol{q}}, \dot{\overline{\boldsymbol{q}}})$ is Coriolis matrix, $\boldsymbol{G} = \boldsymbol{G}(\overline{\boldsymbol{q}})$ represents the gravitational terms and $\overline{\boldsymbol{u}} = [u_1(t)\ u_2(t)]^T \in R^2$ is the vector of motor torques.

$\boldsymbol{D}(\overline{\boldsymbol{q}}) = \begin{bmatrix} m_1 l_{c1}^2 + m_2(l_1^2 + l_{c2}^2 + 2a) & m_2(l_{c1}^2 + a) \\ m_2(l_{c2}^2 + a) & m_2 l_{c2}^2 \end{bmatrix}$ with $a = l_1 l_{c2} \cos q_2$;

$\boldsymbol{C}(\overline{\boldsymbol{q}}, \dot{\overline{\boldsymbol{q}}}) = \begin{bmatrix} h\dot{q}_2 & h(\dot{q}_1 + \dot{q}_1) \\ -h\dot{q}_1 & 0 \end{bmatrix}$ with $h = -m_2 l_1 l_{c2} sinq_2$;

and $\boldsymbol{G}(\overline{\boldsymbol{q}}) = \begin{bmatrix} gcosq_1(m_1 l_{c1} + m_2 l_1 + m_2 g l_{c2} \cos(q_1 + q_2)) \\ m_2 g l_{c2} \cos(q_1 + q_2) \end{bmatrix}$,

where l_{ci} is the distance from the joint i to the center of mass for link a, m_i is the mass of link is, l_i is the length of link i, i=1, 2.

3.0 CONTROL DESIGN FOR SEA

In this section, the dynamic surface control [23] based on backstepping technique (DSC-BC) is described. The design steps are similar to those of backstepping controller, but in order to avoid the need to take derivatives in the iteration steps for the virtual control signal, a low–pass filter has added to the system, both to obtain information about the medium derivative, and to filter out the high – frequency internal noise that occurs in the control objects.

Supposing that the dynamic model contains uncertain parameters such as:

$$\begin{aligned} (\hat{\boldsymbol{D}} + \tilde{\boldsymbol{D}})\ddot{\overline{\boldsymbol{q}}} + (\hat{\boldsymbol{C}} + \tilde{\boldsymbol{C}})\dot{\overline{\boldsymbol{q}}} + (\hat{\boldsymbol{G}} + \tilde{\boldsymbol{G}}) &= (\hat{\boldsymbol{K}} + \tilde{\boldsymbol{K}})(\overline{\boldsymbol{\theta}} - \overline{\boldsymbol{q}}) \\ (\hat{\boldsymbol{J}} + \tilde{\boldsymbol{J}})\ddot{\overline{\boldsymbol{\theta}}} + (\hat{\boldsymbol{K}} + \tilde{\boldsymbol{K}})(\overline{\boldsymbol{\theta}} - \overline{\boldsymbol{q}}) &= \overline{\boldsymbol{u}} \end{aligned} \tag{4}$$

where

$\boldsymbol{D} = \hat{\boldsymbol{D}} + \tilde{\boldsymbol{D}}$ *is inertial matrix.*
$\boldsymbol{C} = \hat{\boldsymbol{C}} + \tilde{\boldsymbol{C}}$ *is Coriolis matrix.*
$\boldsymbol{G} = \hat{\boldsymbol{G}} + \tilde{\boldsymbol{G}}$ *is gravity matrix.*
$\boldsymbol{J} = \hat{\boldsymbol{J}} + \tilde{\boldsymbol{J}}$ *is the inertial matrix of driver motor.*
$\boldsymbol{K} = \hat{\boldsymbol{K}} + \tilde{\boldsymbol{K}}$ *is spring stiffness matrix.*

In this uncertain model, $\hat{\boldsymbol{D}}, \hat{\boldsymbol{C}}, \hat{\boldsymbol{G}}, \hat{\boldsymbol{J}}, \hat{\boldsymbol{K}}$ are the calculated parameters for the model design and $\tilde{\boldsymbol{D}}, \tilde{\boldsymbol{C}}, \tilde{\boldsymbol{G}}, \tilde{\boldsymbol{J}}, \tilde{\boldsymbol{K}}$ are the difference between the calculated model parameter and the actual parameter, or the uncertain components of the model parameters.

The dynamic equation of SEA robot now becomes:

$$\begin{aligned} \hat{\boldsymbol{D}}\ddot{\overline{\boldsymbol{q}}} + \hat{\boldsymbol{C}}\dot{\overline{\boldsymbol{q}}} + \hat{\boldsymbol{G}} + \Delta\bar{\boldsymbol{\varepsilon}}_q &= \hat{\boldsymbol{K}}(\overline{\boldsymbol{\theta}} - \overline{\boldsymbol{q}}) \\ \hat{\boldsymbol{J}}\ddot{\overline{\boldsymbol{\theta}}} + \hat{\boldsymbol{K}}(\overline{\boldsymbol{\theta}} - \overline{\boldsymbol{q}}) + \Delta\bar{\boldsymbol{\varepsilon}}_\theta &= \overline{\boldsymbol{u}} \end{aligned} \tag{5}$$

where

$$\begin{aligned} \Delta\bar{\boldsymbol{\varepsilon}}_q &= \tilde{\boldsymbol{D}}\ddot{\overline{\boldsymbol{q}}} + \tilde{\boldsymbol{C}}\dot{\overline{\boldsymbol{q}}} + \tilde{\boldsymbol{G}} + \tilde{\boldsymbol{K}}(\overline{\boldsymbol{q}} - \overline{\boldsymbol{\theta}}) \\ \Delta\bar{\boldsymbol{\varepsilon}}_\theta &= \tilde{\boldsymbol{J}}\ddot{\overline{\boldsymbol{\theta}}} + \tilde{\boldsymbol{K}}(\overline{\boldsymbol{\theta}} - \overline{\boldsymbol{q}}) \end{aligned} \tag{6}$$

It is supposed that the uncertain parts are bounded, i.e., $|\Delta\bar{\boldsymbol{\varepsilon}}_q| \leq \delta_q$; $|\Delta\bar{\boldsymbol{\varepsilon}}_\theta| \leq \delta_\theta$ with δ_q and δ_θ are finite values.

Define state variables $\bar{\boldsymbol{x}}_1 = \bar{\boldsymbol{q}}, \bar{\boldsymbol{x}}_2 = \dot{\bar{\boldsymbol{q}}}, \bar{\boldsymbol{x}}_3 = \bar{\boldsymbol{\theta}}, \bar{\boldsymbol{x}}_4 = \dot{\bar{\boldsymbol{\theta}}}$, then the system model can be written as

$$\begin{aligned} \dot{\bar{\boldsymbol{x}}}_1 &= \bar{\boldsymbol{x}}_2 \\ \dot{\bar{\boldsymbol{x}}}_2 &= -\hat{\boldsymbol{D}}^{-1}\left(\hat{\boldsymbol{C}}\bar{\boldsymbol{x}}_2 + \hat{\boldsymbol{G}} + \Delta\bar{\boldsymbol{\varepsilon}}_q + \hat{\boldsymbol{K}}(\bar{\boldsymbol{x}}_1 - \bar{\boldsymbol{x}}_3)\right) \\ \dot{\bar{\boldsymbol{x}}}_3 &= \bar{\boldsymbol{x}}_4 \\ \dot{\bar{\boldsymbol{x}}}_4 &= \hat{\boldsymbol{J}}^{-1}\left(\bar{\boldsymbol{u}} - \hat{\boldsymbol{K}}(\bar{\boldsymbol{x}}_3 - \bar{\boldsymbol{x}}_1) - \Delta\bar{\boldsymbol{\varepsilon}}_\theta\right) \end{aligned} \tag{7}$$

The steps to design DSC based on backstepping technique are as follows:

Step 1: Define $\bar{\boldsymbol{e}}_1 = \bar{\boldsymbol{x}}_{1d} - \bar{\boldsymbol{x}}_1$, with $\bar{\boldsymbol{x}}_{1d}$ is the reference joint angle signal. Then,

$$\dot{\bar{\boldsymbol{e}}}_1 = \dot{\bar{\boldsymbol{x}}}_{1d} - \dot{\bar{\boldsymbol{x}}}_1 = \dot{\bar{\boldsymbol{x}}}_{1d} - \bar{\boldsymbol{x}}_2$$

Choose a Lyapunov candidate function as

$$V_1 = \frac{1}{2}\bar{\boldsymbol{e}}_1^T\bar{\boldsymbol{e}}_1 \tag{8}$$

Then,

$$\dot{V}_1 = \bar{\boldsymbol{e}}_1^T\dot{\bar{\boldsymbol{e}}}_1 = \bar{\boldsymbol{e}}_1\left(\dot{\bar{\boldsymbol{x}}}_{1d} - \bar{\boldsymbol{x}}_2\right)$$

Choose virtual control $\bar{F}_1$ as

$$\bar{\boldsymbol{x}}_2 = \bar{F}_1 = \dot{\bar{\boldsymbol{x}}}_{1d} + c_1\bar{\boldsymbol{e}}_1 \tag{9}$$

Then

$$\dot{V}_1 = -c_1\bar{\boldsymbol{e}}_1^T\bar{\boldsymbol{e}}_1 = -k_1V_1 \leq 0 \tag{10}$$

Step 2: To overcome the "explosion of term" problem, a low pass filter is used. Reference [24] also discusses the uses of a low pass filter to smooth the signal produced by the above equation. However, this design technique, we will leave the function F_1 in the form of a low-pass filter $\bar{F}_1$ with time constant τ_1:

$$\begin{aligned} \tau_1\dot{\boldsymbol{F}}_1 + \boldsymbol{F}_1 &= \bar{\boldsymbol{F}}_1 \\ \bar{\boldsymbol{F}}_1(0) &= \boldsymbol{F}_1(0) \end{aligned} \tag{11}$$

Define an error:

$$\Delta\boldsymbol{F}_1 = \boldsymbol{F}_1 - \bar{\boldsymbol{F}}_1 \tag{12}$$

In addition, define:

$$\bar{\gamma}_1 = \frac{d}{dt}\left(-c_1\bar{\boldsymbol{e}}_1 - \dot{\bar{\boldsymbol{x}}}_{1d}\right) \tag{13}$$

Assuming $\bar{\gamma}_1$is bounded by M_1, i.e., $\bar{\gamma}_1 \leq M_1$ with $M_1 > 0$, then $\Delta\dot{\boldsymbol{F}}_1$ is written as:

$$\Delta\dot{\boldsymbol{F}}_1 = -\frac{\Delta\boldsymbol{F}_1}{\tau_1} + \bar{\gamma}_1 \tag{14}$$

Choose a Lyapunov candidate function $V_{F_1} = \frac{1}{2}\Delta\boldsymbol{F}_1^T\Delta\boldsymbol{F}_1$, then:

$$\dot{V}_{F_1} = \Delta\boldsymbol{F}_1^T\Delta\dot{\boldsymbol{F}}_1 = \Delta\boldsymbol{F}_1^T\left(-\frac{\Delta\boldsymbol{F}_1}{\tau_1} + \gamma_1\right) = -\frac{\Delta\boldsymbol{F}_1^T\Delta\boldsymbol{F}_1}{\tau_1} + \Delta\boldsymbol{F}_1\bar{\gamma}_1$$

$$\dot{V}_{F_1} = -\frac{\Delta\boldsymbol{F}_1^T\Delta\boldsymbol{F}_1}{\tau_1} - \frac{1}{2}\left(\frac{\bar{\gamma}_1\Delta\boldsymbol{F}_1}{\sqrt{\sigma_1}} - \sqrt{\sigma_1}\right)^T\left(\frac{\bar{\gamma}_1\Delta\boldsymbol{F}_1}{\sqrt{\sigma_1}} - \sqrt{\sigma_1}\right) + \frac{\bar{\gamma}_1^T\bar{\gamma}_1\Delta\boldsymbol{F}_1^T\Delta\boldsymbol{F}_1}{2\sigma_1} + \frac{\sigma_1}{2}$$

Since $\gamma_1 \leq M_1, M_1 > 0$, then

$$\begin{aligned} \dot{V}_{F1} &\leq -\frac{\Delta\boldsymbol{F}_1^T\Delta\boldsymbol{F}_1}{\tau_1} - \frac{1}{2}\left(\frac{\bar{\gamma}_1\Delta\boldsymbol{F}_1}{\sqrt{\sigma_1}} - \sqrt{\sigma_1}\right)^T\left(\frac{\bar{\gamma}_1\Delta\boldsymbol{F}_1}{\sqrt{\sigma_1}} - \sqrt{\sigma_1}\right) + \frac{M_1^2\Delta\boldsymbol{F}_1^T\Delta\boldsymbol{F}_1}{2\sigma_1} + \frac{\sigma_1}{2} \\ &= -\Delta\boldsymbol{F}_1^T\Delta\boldsymbol{F}_1\left(\frac{1}{\tau_1} - \frac{M_1^2}{2\sigma_1}\right) - \frac{1}{2}\left(\frac{\bar{\gamma}_1\Delta\boldsymbol{F}_1}{\sqrt{\sigma_1}} - \sqrt{\sigma_1}\right)^T\left(\frac{\bar{\gamma}_1\Delta\boldsymbol{F}_1}{\sqrt{\sigma_1}} - \sqrt{\sigma_1}\right) + \frac{\sigma_1}{2} \end{aligned} \tag{15}$$

By choosing τ_1 such as

$$\frac{1}{\tau_1} = \frac{M_1^2}{2\sigma_1} + k_{F1}, \qquad k_{F1} \geq 0 \tag{16}$$

with $\sigma_1 > 0$ can be chosen as small as desired. One can obtain:

$$\dot{V}_{F_1} \leq -k_{F1}\Delta\boldsymbol{F}_1^T\Delta\boldsymbol{F}_1 + \frac{\sigma_1}{2} = -2k_{F1}V_{F_1} + \frac{\sigma_1}{2} \tag{17}$$

Step 3: To realize $\bar{\boldsymbol{x}}_2 \rightarrow \boldsymbol{F}_1$, we define a new error:

$$\bar{\boldsymbol{e}}_2 = \boldsymbol{F}_1 - \bar{\boldsymbol{x}}_2$$

Then

$$\dot{\bar{\boldsymbol{e}}}_2 = \dot{\boldsymbol{F}}_1 - \dot{\bar{\boldsymbol{x}}}_2 = \dot{\boldsymbol{F}}_1 + \hat{\boldsymbol{D}}^{-1}\left(\hat{\boldsymbol{C}}\bar{\boldsymbol{x}}_2 + \hat{\boldsymbol{G}} + \Delta\bar{\boldsymbol{\varepsilon}}_q + \hat{\boldsymbol{K}}(\bar{\boldsymbol{x}}_1 - \bar{\boldsymbol{x}}_3)\right)$$

Choose a Lyapunov candidate function as

$$V_2 = \frac{1}{2}\bar{\boldsymbol{e}}_2^T\bar{\boldsymbol{e}}_2 \tag{18}$$

Then

$$\dot{V}_2 = \bar{\boldsymbol{e}}^T{}_2\dot{\bar{\boldsymbol{e}}}_2 = \bar{\boldsymbol{e}}_2\left(\dot{F}_1 + \hat{D}^{-1}\left(\hat{C}\bar{\boldsymbol{x}}_2 + \hat{G} + \Delta\bar{\boldsymbol{\varepsilon}}_q + \hat{K}(\bar{\boldsymbol{x}}_1 - \bar{\boldsymbol{x}}_3)\right)\right)$$

Choose a virtual control $\bar{\boldsymbol{F}}_2$ as

$$\bar{\boldsymbol{x}}_{\boldsymbol{3}} = \bar{\boldsymbol{F}}_2 = \bar{\boldsymbol{x}}_{\boldsymbol{1}} + \hat{\boldsymbol{K}}^{-1}\big(\hat{\boldsymbol{D}}\big(\dot{\boldsymbol{F}}_1 + c_2\bar{\boldsymbol{e}}_{\boldsymbol{2}}\big) + \hat{\boldsymbol{C}}\bar{\boldsymbol{x}}_{\boldsymbol{2}} + \hat{\boldsymbol{G}} + \delta_q sgn(\bar{\boldsymbol{e}}_{\boldsymbol{2}})\big) \quad (19)$$

Then we would have

$$\dot{V}_2 = -c_2\bar{\boldsymbol{e}}_{\boldsymbol{2}}^{\boldsymbol{T}}\bar{\boldsymbol{e}}_{\boldsymbol{2}} + \hat{\boldsymbol{D}}^{-1}\bar{\boldsymbol{e}}_{\boldsymbol{2}}\Delta\bar{\boldsymbol{\varepsilon}}_q - \hat{D}^{-1}\delta_q|\bar{\boldsymbol{e}}_{\boldsymbol{2}}|$$

Since $|\Delta\bar{\boldsymbol{\varepsilon}}_q| \le \delta_q \Rightarrow \hat{D}^{-1}\bar{\boldsymbol{e}}_{\boldsymbol{2}}\Delta\bar{\boldsymbol{\varepsilon}}_q \le \hat{D}^{-1}\delta_q|\bar{\boldsymbol{e}}_{\boldsymbol{2}}|$, thus

$$\dot{V}_2 \le -c_2\bar{\boldsymbol{e}}_{\boldsymbol{2}}^{\boldsymbol{T}}\bar{\boldsymbol{e}}_{\boldsymbol{2}} = -k_2V_2 \le 0$$

Using (11), the virtual control $\bar{\boldsymbol{F}}_2$ can be calculated as

$$\bar{\boldsymbol{x}}_{\boldsymbol{3}} = \bar{\boldsymbol{F}}_2 = \bar{\boldsymbol{x}}_{\boldsymbol{1}} + \hat{\boldsymbol{K}}^{-1}\left(\hat{\boldsymbol{D}}\left(\frac{\bar{\boldsymbol{F}}_1 - \boldsymbol{F}_1}{\tau_1} + c_2\bar{\boldsymbol{e}}_{\boldsymbol{2}}\right) + \hat{\boldsymbol{C}}\bar{\boldsymbol{x}}_{\boldsymbol{2}} + \hat{\boldsymbol{G}} + \delta_q sgn(\bar{\boldsymbol{e}}_{\boldsymbol{2}})\right) \quad (20)$$

Thus, the derivative component is eliminated.

Step 4: To overcome the "explosion of term" problem, a low pass filter with time constant τ_2 is used as follows:

$$\tau_2\dot{\boldsymbol{F}}_2 + \boldsymbol{F}_2 = \bar{\boldsymbol{F}}_2 \qquad \bar{\boldsymbol{F}}_2(0) = \boldsymbol{F}_2(0) \quad (21)$$

We define an error:

$$\Delta\boldsymbol{F}_2 = \boldsymbol{F}_2 - \bar{\boldsymbol{F}}_2 \quad (22)$$

In addition, define:

$$\bar{\gamma}_2 = \frac{d}{dt}\big(-\hat{\boldsymbol{K}}^{-1}\big(\hat{\boldsymbol{D}}\big(\dot{\boldsymbol{F}}_1 + c_2\bar{\boldsymbol{e}}_{\boldsymbol{2}}\big) + \hat{\boldsymbol{C}}\bar{\boldsymbol{x}}_{\boldsymbol{2}} + \hat{\boldsymbol{G}} + \delta_q sgn(\bar{\boldsymbol{e}}_{\boldsymbol{2}})\big)\dot{\bar{\boldsymbol{x}}}_{\boldsymbol{1d}}\big) \quad (23)$$

Assuming that $\bar{\gamma}_2$ is bounded by M_2, i.e., $\bar{\gamma}_2 \le M_2, M_2 > 0$, then $\Delta\dot{F}_2$ is written as:

$$\Delta\dot{\boldsymbol{F}}_2 = -\frac{\Delta\boldsymbol{F}_2}{\tau_2} + \bar{\gamma}_2 \quad (24)$$

And we choose a Lyapunov candidate function $V_{F_2} = \frac{1}{2}\Delta\boldsymbol{F}_2^T\Delta\boldsymbol{F}_2$. Similar to step 2, by choosing τ_2 such as

$$\frac{1}{\tau_2} = \frac{M_2^2}{2\sigma_2} + k_{F2}, \qquad k_{F2} \ge 0 \quad (25)$$

with $\sigma_2 > 0$ can be chosen as small as desired. Then we have

$$\dot{V}_{F_2} \le -k_{F2}\Delta\boldsymbol{F}_2^T\Delta\boldsymbol{F}_2 + \frac{\sigma_2}{2} = -2k_{F2}V_{F_1} + \frac{\sigma_2}{2} \quad (26)$$

Step 5: To realize $\bar{\boldsymbol{x}}_{\boldsymbol{3}} \to \boldsymbol{F}_2$, we get a new error:

$$\bar{\boldsymbol{e}}_{\boldsymbol{3}} = \boldsymbol{F}_2 - \bar{\boldsymbol{x}}_{\boldsymbol{3}}$$

Then $\dot{\bar{\boldsymbol{e}}}_{\boldsymbol{3}} = \dot{\boldsymbol{F}}_2 - \dot{\bar{\boldsymbol{x}}}_{\boldsymbol{3}} = \dot{\boldsymbol{F}}_2 - \bar{\boldsymbol{x}}_{\boldsymbol{4}}$,

Select the Lyapunov function as

$$V_3 = \frac{1}{2}\bar{\boldsymbol{e}}_{\boldsymbol{3}}^{\boldsymbol{T}}\bar{\boldsymbol{e}}_{\boldsymbol{3}} \quad (27)$$

Then

$$\dot{V}_3 = \bar{\boldsymbol{e}}_{\boldsymbol{3}}\dot{\bar{\boldsymbol{e}}}_{\boldsymbol{3}} = \bar{\boldsymbol{e}}_{\boldsymbol{3}}\big(\dot{\boldsymbol{F}}_2 - \bar{\boldsymbol{x}}_{\boldsymbol{4}}\big)$$

Choose virtual control as:

$$\bar{\boldsymbol{x}}_{\boldsymbol{4}} = \bar{\boldsymbol{F}}_3 = \dot{\boldsymbol{F}}_2 + c_3\bar{\boldsymbol{e}}_{\boldsymbol{3}} \quad (28)$$

Then,

$$\dot{V}_3 = -c_3\bar{\boldsymbol{e}}_{\boldsymbol{3}}^{\boldsymbol{T}}\bar{\boldsymbol{e}}_{\boldsymbol{3}} = -k_3V_3 \le 0 \quad (29)$$

Using (21), the virtual control $\bar{F}_3$ can be calculated as

$$\bar{\boldsymbol{x}}_{\boldsymbol{4}} = \bar{\boldsymbol{F}}_3 = \frac{\bar{\boldsymbol{F}}_2 - \boldsymbol{F}_2}{\tau_2} + c_3\bar{\boldsymbol{e}}_{\boldsymbol{3}} \quad (30)$$

Thus, the derivative component is eliminated.

Step 6: To overcome the "explosion of term" problem, a low pass filter with time constant τ_3 is used as follows:

$$\tau_3\dot{\boldsymbol{F}}_3 + \boldsymbol{F}_3 = \bar{\boldsymbol{F}}_3 \qquad \bar{\boldsymbol{F}}_3(0) = \boldsymbol{F}_3(0) \quad (31)$$

We define an error:

$$\Delta\boldsymbol{F}_3 = \boldsymbol{F}_3 - \bar{\boldsymbol{F}}_3 \quad (32)$$

In addition, define:

$$\bar{\gamma}_3 = \frac{d}{dt}\big(-\dot{\boldsymbol{F}}_2 - c_3\bar{\boldsymbol{e}}_{\boldsymbol{3}}\big) \quad (33)$$

Assuming that $\bar{\gamma}_3$ is bounded by M_3, i.e.,$\bar{\gamma}_3 \le M_3, M_3 > 0$, then $\Delta\dot{\boldsymbol{F}}_3$ is written as:

$$\Delta\dot{\boldsymbol{F}}_3 = -\frac{\Delta\boldsymbol{F}_3}{\tau_3} + \bar{\gamma}_3 \quad (34)$$

And we choose a Lyapunov candidate function $V_{F_3} = \frac{1}{2}\Delta\boldsymbol{F}_3^T\Delta\boldsymbol{F}_3$. Similar to step 2, by choosing τ_3 such as

$$\frac{1}{\tau_3} = \frac{M_3^2}{2\sigma_3} + k_{F3}, \qquad k_{F3} \ge 0 \quad (35)$$

with $\sigma_3 > 0$ can be chosen as small as desired. Then we have

$$\dot{V}_{F_3} \le -k_{F3}\Delta\boldsymbol{F}_3^T\Delta\boldsymbol{F}_3 + \frac{\sigma_3}{2} = -2k_{F3}V_{F_3} + \frac{\sigma_3}{2} \quad (36)$$

Step 7: To realize $\bar{\boldsymbol{x}}_4 \to \boldsymbol{F}_3$, we get a new error:

$$\bar{\boldsymbol{e}}_4 = \boldsymbol{F}_3 - \bar{\boldsymbol{x}}_4$$

Then, $\dot{\bar{\boldsymbol{e}}}_4 = \dot{\boldsymbol{F}}_3 - \dot{\bar{\boldsymbol{x}}}_4 = \dot{\boldsymbol{F}}_3 - \hat{\boldsymbol{J}}^{-1}\left(\bar{\boldsymbol{u}} - \hat{\boldsymbol{K}}(\bar{\boldsymbol{x}}_3 - \bar{\boldsymbol{x}}_1) - \Delta\bar{\boldsymbol{\varepsilon}}_\theta\right)$

Choose a Lyapunov candidate function as

$$V_4 = \frac{1}{2}\bar{\boldsymbol{e}}_4^T\bar{\boldsymbol{e}}_4 \tag{37}$$

Then

$$\dot{V}_4 = \bar{\boldsymbol{e}}_4^T\dot{\bar{\boldsymbol{e}}}_4 = \bar{\boldsymbol{e}}_4\left(\dot{\boldsymbol{F}}_3 - \hat{J}^{-1}\left(\bar{\boldsymbol{u}} - \hat{\boldsymbol{K}}(\bar{\boldsymbol{x}}_3 - \bar{\boldsymbol{x}}_1) - \Delta\bar{\boldsymbol{\varepsilon}}_\theta\right)\right)$$

Choose the control law:

$$\bar{\boldsymbol{u}} = \hat{\boldsymbol{J}}\left(\dot{\boldsymbol{F}}_3 + c_4\bar{\boldsymbol{e}}_4\right) + \hat{\boldsymbol{K}}(\bar{\boldsymbol{x}}_3 - \bar{\boldsymbol{x}}_1) + \delta_\theta sgn(\bar{\boldsymbol{e}}_4) \tag{38}$$

Then

$$\dot{V}_4 = \bar{\boldsymbol{e}}_4\left(-c_4\bar{\boldsymbol{e}}_4 - \hat{J}^{-1}(\delta_\theta sgn(\bar{\boldsymbol{e}}_4) - \Delta\bar{\boldsymbol{\varepsilon}}_\theta)\right) = -c_4\bar{\boldsymbol{e}}_4^T\bar{\boldsymbol{e}}_4 - \hat{J}^{-1}(\delta_\theta|\bar{\boldsymbol{e}}_4| - \bar{\boldsymbol{e}}_4\Delta\bar{\boldsymbol{\varepsilon}}_\theta)$$

Since$|\Delta\bar{\boldsymbol{\varepsilon}}_\theta| \le \delta_\theta \Longrightarrow \bar{\boldsymbol{e}}_4\Delta\bar{\boldsymbol{\varepsilon}}_\theta \le \delta_\theta|\bar{\boldsymbol{e}}_4|$. Thus,

$$\dot{V}_4 \le -c_4\bar{\boldsymbol{e}}_4^T\bar{\boldsymbol{e}}_4 = -k_4V_4 \le 0 \tag{39}$$

Using (21), the control signal $\bar{\boldsymbol{u}}$ can be calculated as

$$\bar{\boldsymbol{u}} = \hat{\boldsymbol{J}}\left(\frac{\bar{\boldsymbol{F}}_3 - \boldsymbol{F}_3}{\tau_3} + c_4\bar{\boldsymbol{e}}_4\right) + \hat{\boldsymbol{K}}(\bar{\boldsymbol{x}}_3 - \bar{\boldsymbol{x}}_1) + \delta_\theta sgn(\bar{\boldsymbol{e}}_4) \tag{40}$$

Thus, the derivative component is eliminated.

Step 8:

Choose the Lyapunov candidate function:

$$V = V_1 + V_{F1} + V_2 + V_{F2} + V_3 + V_{F3} + V_4 \tag{41}$$

Then

$$\dot{V} = \dot{V}_1 + \dot{V}_{F1} + \dot{V}_2 + \dot{V}_{F2} + \dot{V}_3 + \dot{V}_{F3} + \dot{V}_4$$

According to (9), (16), (19), (26), (29), (36), and (39) one can obtain:

$$\dot{V} \le -k_1V_1 - 2k_{F1}V_{F1} - k_2V_2 - V_{F2} - k_3V_3 - 2k_{F3}V_{F3} - k_4V_4 + \frac{\sigma_1}{2} + \frac{\sigma_2}{2} + \frac{\sigma_3}{2} \le -kV + \sigma$$

where $k = \min\{k_1, 2k_{F1}, k_2, 2k_{F2}, k_3, 2k_{F3}, k_4\}$ and $\sigma = \frac{\sigma_1}{2} + \frac{\sigma_2}{2} + \frac{\sigma_3}{2}$.

Since $\dot{V} \le -kV + \sigma$, it can be concluded that V, and therefore the tracking errors, will be confined to a ball of radius σ that can be made as small as desired.

Based on the above proof, we can give the proposed control structure as in Figure 2.

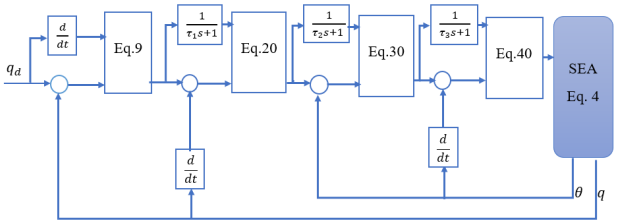

Figure 2. Controller structure of SEA

4.0 SIMULATIONS

In this paper, to validate the proposed control algorithm, simulation is done. The simulation parameters are chosen as in Table 1.

Table 1. Model parameter of SEA

Parameter	Joint	
	Joint 1	Joynt
$\boldsymbol{K}\left(\frac{N}{m}\right)$	$K_1 = 40$	$K_2 = 30$
$l\ (m)$	$l_1 = 0.25$	$l_2 = 0.25$
$l_c\ (m)$	$l_{c1} = 0.125$	$l_{c1} = 0.125$
$m\ (kg)$	$m_1 = 2.35$	$m_2 = 1.53$
$\boldsymbol{J}\left(\frac{kg}{m^2}\right)$	$J_1 = 0.0185$	$J_2 = 0.0185$

Suppose we control the robot running from the first position $q_0 = [0\ 0]$ (rad) to move along the trajectory $2 - 1 - 2$ to position $q_c = [2.4\ 2.6]$ (rad). After adjusting the parameters, we simulate and make the comparison between Dynamic surface control based on backstepping controller (DSC-BC) and conventional backstepping controller (BC). Two situations are considered. In the first case, there is no parameter error, i.e., the robot parameters are all known precisely. And in the second case, all the system parameter values, except motor inertia, that are used to calculate the control input, are 20% different from the actual system parameters, i.e., the parameter values are used to simulate the system.

4.1 The SEA in Case of No Parameter Error

The simulation results of both DSC-BC and BC are shown in Figures 3 and Figure 4. From the simulation results, both controllers can successfully achieve the desired position and speed trajectory responses with small errors. In the case of BC,

the maximum position error for joint 1 and joint 2 are 0.0012 (rad) and 0.003 (rad), respectively. In the case of DSC-BC, the maximum position error is much smaller. The maximum position error for joint 1 and joint 2 are 0.0007 (rad) and 0.0005 (rad), respectively. In addition, the DSC-BC outperforms the BC in several aspects. One limitation BC is the occurrence of large derivative variations, also known as the "explosion of terms." These variations can lead to unstable control behavior and negatively impact system performance. By incorporating DSC, the controller effectively mitigates these variations by introducing a dynamic surface that regulates the control signal's rate of change. This ensures smoother and more stable control action throughout the system.

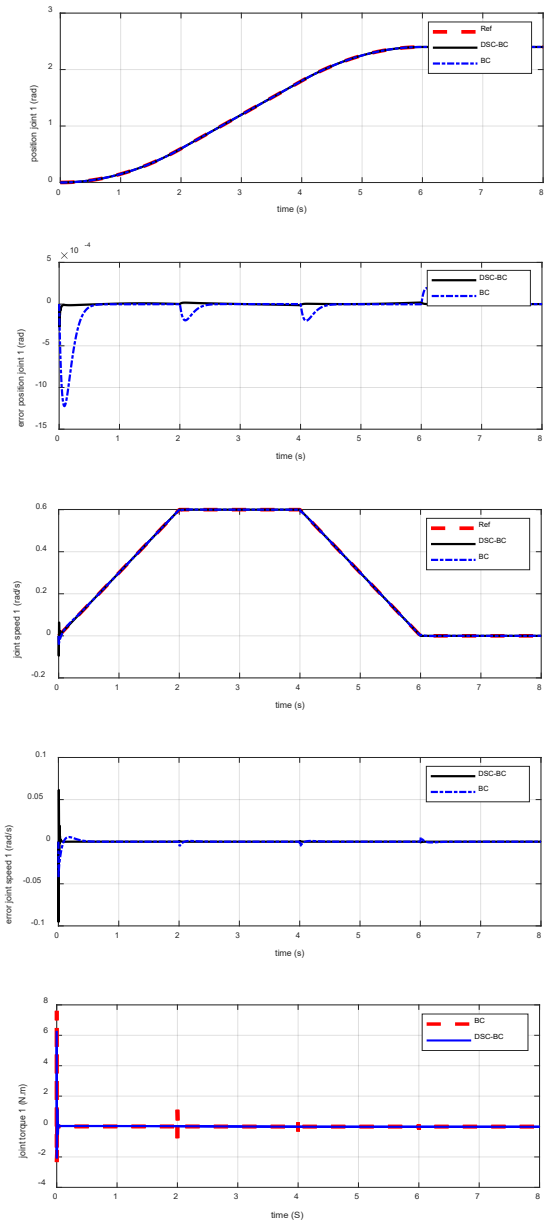

Figure 3. The simulation results joint 1 without parameter error

Furthermore, the DSC controller demonstrates superior performance in suppressing chattering phenomena. Chattering refers to rapid and irregular fluctuations in the control signal, which can introduce unnecessary control actions and degrade system efficiency. Thanks to its inherent design characteristics and low-pass filtering properties, the DSC controller effectively reduces chattering, resulting in a more refined and continuous control action.

In summary, while both controllers can achieve satisfactory position and speed trajectory responses, the utilization of the DSC controller offers notable advantages over the pure backstepping technique. By addressing the limitations associated with large derivative variations and chattering, the DSC controller ensures smoother and more stable control performance, ultimately enhancing the overall efficiency of the system.

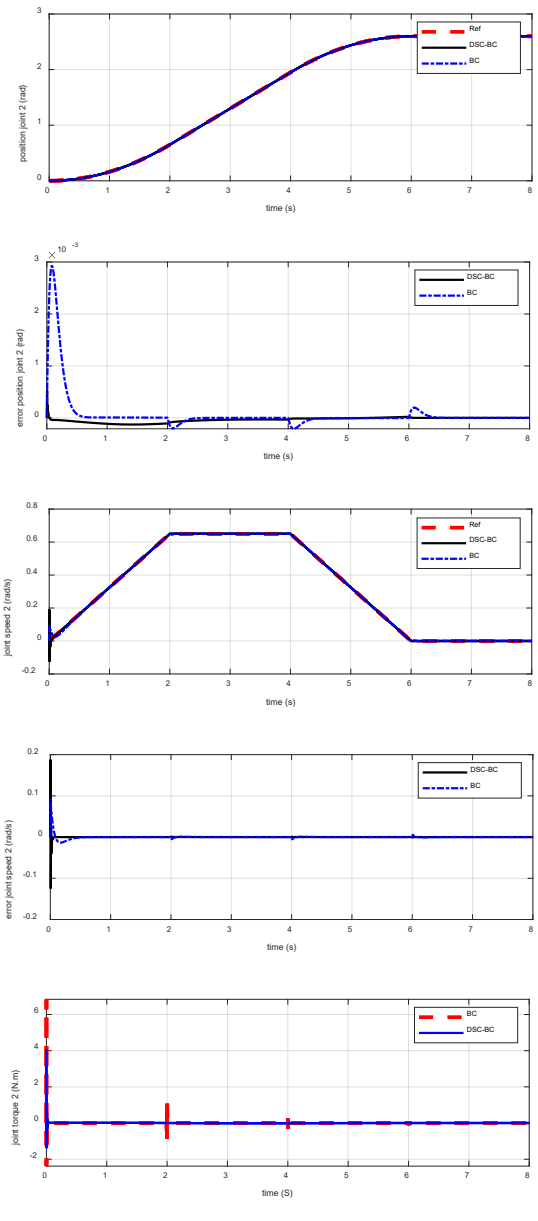

Figure 4. The simulation results joint 2 without parameter error

4.2 The SEA In Case Of 20% Parameter Error

To further validate the effectiveness of the proposed DSC-BC controller, the simulation with 20% parameter error is done with both DSC-BC and BC controllers. The simulation results are shown in Figures 5 and 6. In this case, both DSC-BC and BC controllers still can keep the system stability, but the system performance is degraded.

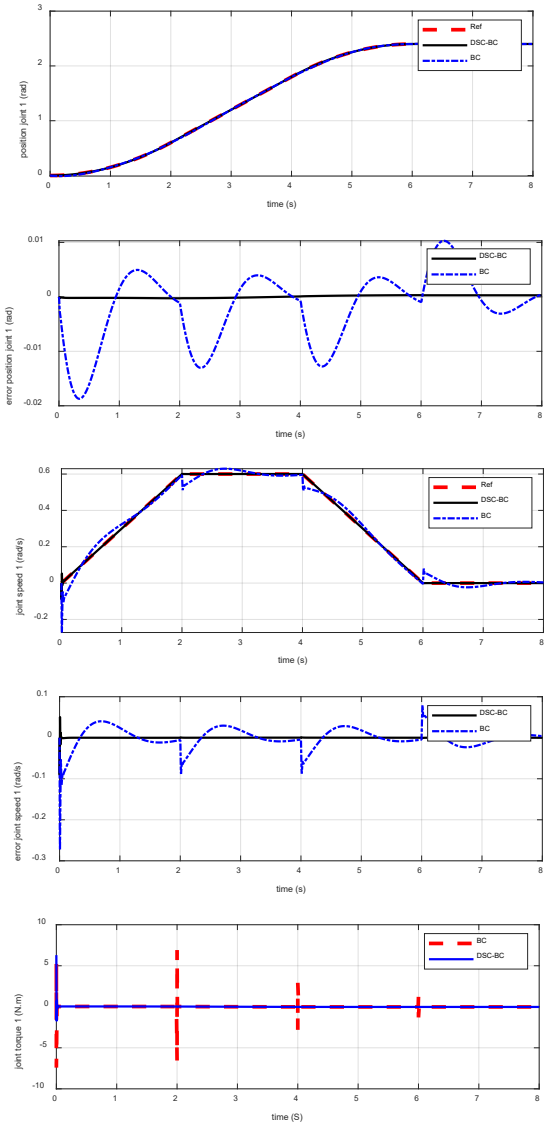

Figure 5. The simulation results joint 1 with 20% parameter error

For DSC-BC, the degradation is relatively insignificant, the maximum position error of joint 1 and joint 2 are 0.0012 (rad) and 0.003 (rad), respectively. While with the BC, the maximum position error of joint 1 and joint 2 are 0.0185 (rad) and 0.026 (rad), respectively. DSC-BC has shown its capability in handling unknown components within the system model. In addition, the maximum control input in case of DSC-BC is 6 (Nm) for joint 1 and 4 (Nm) for joint 2. While the maximum control input in case of BC is larger, 6.5 (Nm) for joint 1 and 5.6 (Nm) for joint 2. This advantage of DSC-BC comes from the use of a low-pass filter that effectively smooths the signal. Consequently, DSC-BC improved stability and provides more accurate position tracking, in comparison to BC.

The simulation with up to 50% parameter error has also been done. The system with DSC-BC is still stable, but the performance is reduced significantly. When the error increases, the system stability may not be guaranteed.

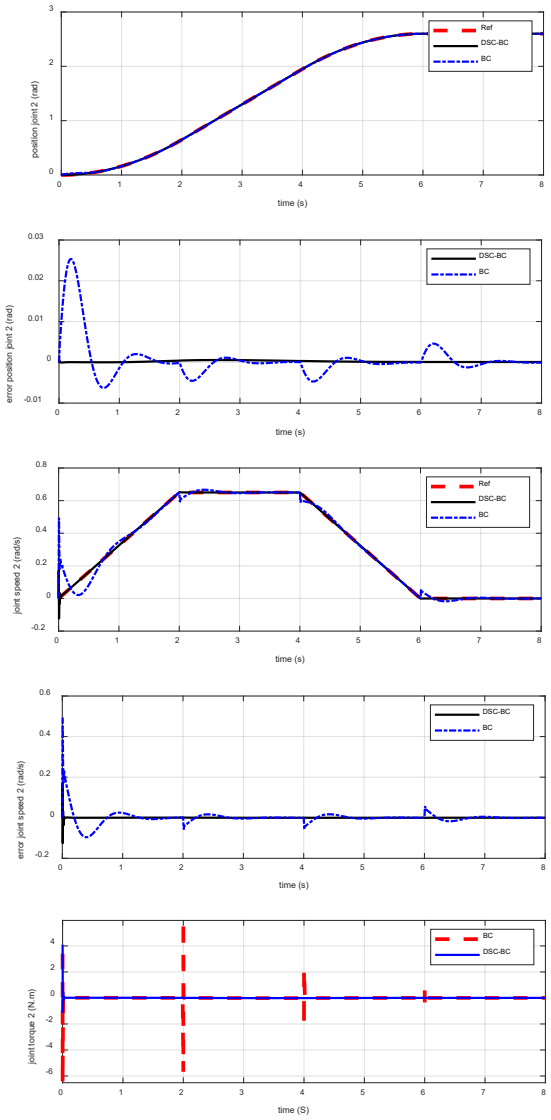

Figure 6. The simulation results joint 2 with 20% parameter error

5.0 CONCLUSION

In this paper, dynamic surface control based backstepping technique has been proposed. It is shown that DSC-BC can handle unknown components in the system model, and it also overcomes the limitations of the large derivative variation "explosion of terms", and chattering is better when using a controller using pure backstepping technique. The DSC-BC algorithm gives a better response than the pure backstepping controller in the case when the system contains uncertain components.

Accordingly, the use of DSC-BC helps the system to be stable against interference. This can be considered as one of the basic solutions for SEA when the system contains unknown parameters. However, the DSC-BC controller still has certain disadvantages that are difficult to respond to unknow parameter with large variation. In the future the adaptive DSC-BC will be considered.

Acknowledgement

This work was supported by Hanoi University of Science and Technology. The authors would also like to express their gratitude to whosoever had contributed to their work either directly or indirectly.

References

[1] Robinson, D. W. 2000. Design and analysis of series elasticity in closed-loop actuator force control. PhD Thesis, Massachusetts Institute of Technology.

[2] Pratt, G. A. 1995. Williamson, Stiffness isn't everything. *Proc. 4th Int. Symp. on Experimental Robotics*. 173–178. DOI: 10.1007/BFb0035216

[3] Pratt, J., and B. Krupp. 2008. Design of a bipedal walking robot. *Unmanned systems technology X*. SPIE. 480–492. DOI: 10.1117/12.777973

[4] Pratt, J. E. 1995. Virtual model control of a biped walking robot. M.Eng. Thesis, Department of Electrical Engineering and Computer Science, Massachusetts Institute of Technology.

[5] Zinn, M., B. Roth, O. Khatib, and J. K. Salisbury. 2004. A new actuation approach for human friendly robot design. *The international journal of robotics research*. 23(4–5): 379–398. DOI: 10.1109/ROBOT.2004.1307159

[6] Howard, R. D. 1990. Joint and actuator design for enhanced stability in robotic force control. PhD Thesis, Massachusetts Institute of Technology.

[7] Raibert, M. H. 1986. *Legged robots that balance*. MIT press.

[8] Koditschek, D. E, and M. Bühler. 1991. Analysis of a Simplified Hopping Robot. *The International Journal of Robotics Research*. 10(6):587-605. DOI:10.1177/027836499101000601

[9] Brown, B., and G. Zeglin. 1998. The bow leg hopping robot. *Proceedings. 1998 IEEE International Conference on Robotics and Automation.* 781–786. DOI: 10.1109/ROBOT.1998.677072

[10] Pratt, G. A., and M. M. Williamson. 1995. Series elastic actuators. *Proceedings 1995 IEEE/RSJ International Conference on Intelligent Robots and Systems. Human Robot Interaction and Cooperative Robots*. 1: 399-406. DOI: 10.1109/IROS.1995.525827

[11] Yu, H., S. Huang, G. Chen, Y. Pan, and Z. Guo. 2015. Human–robot interaction control of rehabilitation robots with series elastic actuators. *IEEE Transactions on Robotics*. 31(5): 1089–1100. DOI: 10.1109/TRO.2015.2457314

[12] Isik, K., S. He, J. Ho, and L. Sentis. 2017. Re-engineering a high performance electrical series elastic actuator for low-cost industrial applications. *Actuators*. MDPI. 5. DOI: 10.3390/act6010005

[13] Lee, H., J. Lee, J.-H. Ryu, and S. Oh. 2019. Relaxing the conservatism of passivity condition for impedance controlled series elastic actuators. *2019 IEEE/RSJ International Conference on Intelligent Robots and Systems (IROS)*. 7610–7615. DOI: 10.1109/IROS40897.2019.8968217

[14] Sun, H. J., J. Ye, and G. Chen. 2021. Trajectory Tracking of Series Elastic Actuators Using Terminal Sliding Mode Control. *33rd Chinese Control and Decision Conference (CCDC)*. 189–194. DOI: 10.1109/CCDC52312.2021.9601778

[15] Sariyildiz, E., H. Wang, and H. Yu. 2017. A sliding mode controller design for the robust position control problem of series elastic actuators. *2017 IEEE International Conference on Robotics and Automation (ICRA)*. 3055–3061. DOI: 10.1109/ICRA.2017.7989350

[16] Sun, W., L. Sun, M. Wang, S. Lei, and J. Liu. 2016. An integral sliding-mode control approach for series elastic actuator torque control. *2016 IEEE International Conference on Robotics and Biomimetics (ROBIO)*. 1209–1214. DOI: 10.1109/ROBIO.2016.7866490

[17] Zhao, W., L. Sun, W. Yin, M. Li, and J. Liu. 2019. Robust Position Control of Series Elastic Actuator with Backstepping Based on Disturbance Observer. *2019 IEEE/ASME International Conference on Advanced Intelligent Mechatronics (AIM)*. 618–623. DOI: 10.1109/AIM.2019.8868550

[18] Duong, M. D., and T. T. Tung. 2023. Adaptive Slotine - Li based backstepping control for series elastic actuator robot. *Measurement, Control, and Automation*. 4(1): 56-61.

[19] Kenanoglu, C. U., and V. Patoglu. 2022. Passivity of Series Elastic Actuation Under Model Reference Force Control During Null Impedance Rendering. *IEEE Transactions on Haptics*. 15(1): 51–56. DOI: 10.1109/TOH.2021.3140143

[20] Losey, D. P., A. Erwin, C. G. McDonald, F. Sergi, and M. K. O'Malley. 2016. A time-domain approach to control of series elastic actuators: Adaptive torque and passivity-based impedance control. *IEEE/ASME Transactions on Mechatronics*. 21(4): 2085–2096. DOI: 10.1109/TMECH.2016.2557727.

[21] Lin, Y., Z. Chen, and B. Yao. 2019. Decoupled torque control of series elastic actuator with adaptive robust compensation of time-varying load-side dynamics. *IEEE Transactions on Industrial Electronics.* 67(7): 5604–5614. DOI: 10.1109/TIE.2019.2934023

[22] Spong, M. W., S. Hutchinson, and M. Vidyasagar. 2006. *Robot modeling and control*. New York: Wiley.

[23] Swaroop, D., J. K. Hedrick, P. P. Yip and J. C. Gerdes. 2000. Dynamic surface control for a class of nonlinear systems. *IEEE Transactions on Automatic Control*. 45(10): 1893-1899. DOI: 10.1109/TAC.2000.880994.

[24] Green, J. H., and J. K. Hedrick. 1990. Nonlinear speed control for automotive engines. *1990 American Control Conference*, IEEE. 2891–2897. DOI: 10.23919/ACC.1990.4791247